International Journal of Concrete Structures and Materials

RESEARCH Open Access

Experimental Verification of Modal Identification of a High-rise Building Using Independent Component Analysis

Jae-Seung Hwang[1], Jung-Tae Noh[2], Sang-Hyun Lee[3*] and Ahsan Kareem[4]

Abstract

Independent component analysis is one of the linear transformation methods based the techniques for separating blind sources from the output signals of the system. Recently, the method has been analytically applied to the identification of mode shapes and modal responses from the output signal of structures. This study aims to experimentally validate the blind source separation using ICA method and propose a novel method for identification of the modal parameters from the decomposed modal responses. The result of the experimental testing on the three-story steel scale model shows that the mode shapes obtained by ICA method are in good agreement with those by the analytical and peak-picking method in the frequency domain. Based on the robust mathematical model, ICA can calculate the natural frequency and damping ratio effectively using the probability distribution function of the instantaneous natural frequency determined by Hilbert transform of the decomposed modal responses and the change in the output covariance. Finally, the validity of the proposed method paves the way for more effective output-only modal identification for assessment of existing steel-concrete buildings.

Keywords: independent component analysis, mode decomposition, Hilbert transform, instantaneous natural frequency, derivative of covariance, output-only modal analysis

1 Introduction

Modal parameters are vital to understand the structure's behavior. By decomposing the global response into the equivalent SDOF system's responses corresponding to each mode, the mode shape, natural frequency and damping can be estimated. The modal parameters of existing buildings are employed to update and refine the numerical model for structural analysis and, subsequently, enable localization and assessment of the damage by comparing pre-and post-damage state (Alvandi and Cremona 2006). As for calculating the effective mass of the damper and the input for control algorithm of the active mass damper, the dynamic identification technique is of great importance. For these reasons, a number of modal identification methods have been studied and applied to many fields of engineering. The recent advance of structural health monitoring also encouraged development of Operational Modal Analysis for maintenance of existing buildings using ambient vibration (Zhang and Brincker 2005; Reynders 2012). OMA, also referred to as Output-only Modal Analysis based on mathematical robustness is extensively being exploited to determine the dynamic parameters of structures using only the ambient vibration as input. The classical frequency-domain techniques that employ the contribution ratio of the specific mode to the overall output at the sensor locations are widely used (Brincker et al. 2002). However, the frequency-domain technique has intrinsic uncertainty in the identification of modal parameters since determining modal participation ratio relies on engineer's decision. One of most well-known methods, Stochastic subspace identification is based on the assumption that the external excitation is represented as a white noise and the variable in its procedure such as determining the order of the

*Correspondence: lshyun00@dankook.ac.kr
[3] Department of Architectural Engineering, Dankook University, 152, Jukjeon-ro, Suji-gu, Yongin-Si, Gyeonggi-do 16890, Republic of Korea
Full list of author information is available at the end of the article
Journal information: ISSN 1976-0485 / eISSN 2234-1315

system relying on engineering judgement also leads to uncertainties (Peeters and De Roeck 1999). Other recent development in system identification schemes involving structural health monitoring may be found in (Guo and Kareem 2015, 2016a, b; Guo et al. 2016; Hwang et al. 2018).

Principal Component Analysis is another approach to decompose the response signal into modal responses by the linear transformation of the output. PCA employs the normal orthogonal basis determined by the covariance of structure's response to extract the mode shapes of the structure (Feeny 2002; Han and Feeny 2003). Since PCA also uses the gaussian excitation for input, robustness of linear transform of the method is degraded with respect to non-gaussian excitation and underdetermined case.

Over the last two decades, Independent Component Analysis which is one of the most popular Blind Source Separation techniques has recently become a focused topic of research work due to its high potential in mode decomposition of non-gaussian structural response. ICA was introduced in Lee (1998), Hyvaerinen and Oja (2000), and Hyvaerinen et al. (2001). The method that makes use of cumulative density other than covariance allows one to obtain independent components comprising the structure's response and determine modal parameters at the location of the limited number of sensors. It has recently become the focus of intensive research work due to its high potential in many applications. The extensive application of ICA can be found in image processing (Fortuna and Capson 2002), biomedical data analysis (Cichocki 2004), and telecommunication (Madhow 1998). Several applications in structural dynamics are presented in the literature. Zang et al. (2004) demonstrated the result of simulated damage detection of the truss and frame structure using ICA. Poncelet et al. (2007) presented the robustness of the proposed BSS methods for the simple and moderately damped systems. Zhou and Chelidze (2007) proposed BSS-based mode shape extraction and illustrated its performance by comparing its result to that of the time-domain analysis. Hazra et al. (2010) pointed out the limited performance of ICA under the certain level of damping presence and proposed a new method based on modified cross-correlation. As a statistical measure of independence of the components, kurtosis is usually employed to separate independent components (McNeill and Zimmerman 2010; Wu 2011). However, ICA faces difficulties with closely spaced modes and the highly damped system cases subject to non-stationary ambient excitation. Yang and Nagarajaiah (2013) and Nagarajaiah and Yang (2013) proposed the improved ICA techniques employing complexity pursuit algorithm, short time Fourier transform in time–frequency domain, respectively. The further modification of ICA for the particular case of the non-proportionally damped structures is verified in (Nagarajaiah and Yang 2015).

In most OMA techniques, extracting modal properties other than the mode shape requires a post-process. To address this challenge, revised fixed-point complex ICA is presented in (Yang et al. 2013). Another application of ICA is found in Structural Health monitoring and damage identification. The long-term monitoring response is processed in wavelet-domain before ICA to capture the time varying modal parameters (Yang and Nagarajaiah 2014) and the SHM data is compressed and transferred using Fast ICA algorithm (Yang et al. 2015). The latest development and application of ICA based modal identification methods are summarized in Sadhu et al. (2017).

In this paper, the algorithm of ICA for modal parameters extraction and the experimental modal analysis of the high-rise building subjected to strong wind load is discussed within the ICA framework. Since the analytical approach is limited to be applied to the response containing nonlinearity and low signal-to-noise ratio, the experimental evaluation is crucial to examine the applicability of ICA to the real structure's response.

First, a three-story scale model made of steel elements are used as a preliminary validation of the ICA algorithm. Assuming the input excitation is unknown, the mode decomposition of the response measured at each floor by the accelerometers is carried out. At the same time, the experimental testing shows that the linear combination matrix used in mode decomposition is equivalent to the mode shape of the structure. Subsequently, the natural frequency and damping ratio is obtained from the decomposed modal responses. The same procedure is repeated for the accelerations measured at the top floor of the high-rise building to examine the close modes separation performance of the ICA technique. Lastly, the modal parameters identified by ICA are compared with those by a conventional method.

This paper is organized as follows. The principle of ICA is explained in Sect. 2. Section 3 presents the modal analysis of the scale model and tall building followed by introducing and applying the effective modal parameter extraction method (Lee et al. 2017; Du et al. 2017). In Session 4, finally, the results of the modal analysis on the examples are discussed comparing with other classical dynamic identification methods and the concluding remarks are presented.

2 Basic Principles of ICA

2.1 Fundamentals of ICA

ICA is a linear transformation based on non-Gaussianity of the variables characterized by data independence. The method is an extended Principal Component Analysis as a second order linear transformation using the

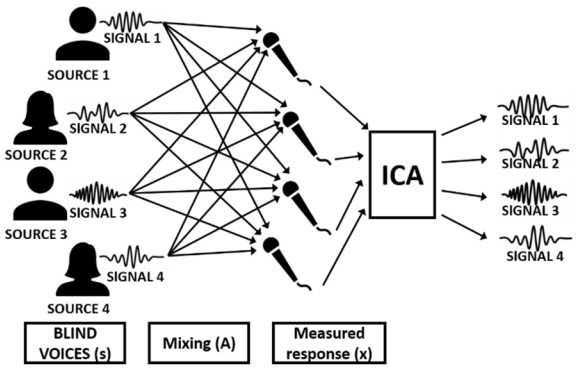

Fig. 1 The schematic drawing of the Cocktail party problem.

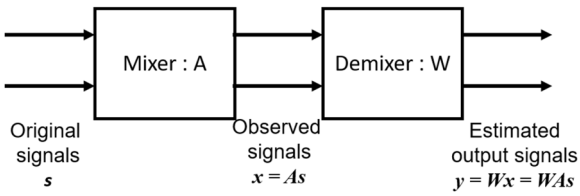

Fig. 2 ICA procedure.

covariance that accounts for the correlation between the gaussian signals. ICA is a process to solve so called the Cocktail-party problem (Bee and Micheyl 2008; Haykin and Chen 2005). For instance, if someone is in a bustling party filled with a great deal of voices from many people, her or his voice is mixed with the other individual voices and recorded by a microphone as shown in Fig. 1. Although the how the individual sounds are mixed is unknown, one can recognize the individual voice of her or his friend. As the human brain works, separating the unique sound from the mixture using only the measured sound is the key idea of ICA. In this sense, the individual sounds and the mixed sound measured by the microphone correspond to independent component and output or response, respectively and ICA is the technique to estimate not only the independent components, but their mixing process simultaneously. If linearly combined input signals are given, ICA can inversely decompose it into statistically independent input signal.

The relation between the mixed signal and input is expressed in the form

$$x = As + \widehat{N} = \sum_{i=1}^{m} s(i)\alpha(i) + \widehat{N} \tag{1}$$

where A represents mixing matrix that is unknown at this point and $\widehat{N}$ is noise. Since the noise can be hardly separated from the input, it is usually neglected. $\alpha(i)$ is basis and component of $A = [\alpha(1), \alpha(2), \ldots\ldots, \alpha(m)]$. In short, ICA is a solution for the inverse matrix A^{-1} using the observed data that is the measured mixed signal x. The procedure of ICA is displayed in Fig. 2. As shown, the observed output of the mixer is available, while the mixing characteristic A and the original input s are unknown. The result of the analysis shall satisfy the fact that the input coincides with the output y,

$$y = Wx = WAs \tag{2}$$

The relation between W and A satisfying the prior condition is given by

$$WA = I, \quad W = A^{-1} \tag{3}$$

It is worth noting that the elements of the output y must be statistically independent to each other and the orthogonality condition does not hold. Consequently, original signal s is approximated by determining W which can be calculated by optimization of its associated objective function. To facilitate the ICA, the pre-processed mixed signal considering the first and second-order statistical correlation is employed.

2.2 Pre-processing of ICA

The signal is subject to zero-mean and whitening process prior to ICA. The former is a normalization method considering the second-order statistics of the observed data and helps the learning algorithm. Meanwhile, the latter is to reduce the dependency on each data and produces more independent data. The zero-mean process of data is defined as

$$x' = x - \bar{x} \tag{4}$$

Whitening is achieved by making the covariance matrix of data vector x identity, namely $E(xx^T) = I$.

One of the widely used whitening methods is the analytical method using PCA and its whitening matrix V is defined as

$$V = D^{(-\frac{1}{2})}E^T \tag{5}$$

where D is the diagonal matrix comprised of eigen values λ and E is the orthogonal matrix comprised of eigen vectors.The advantage of PCA whitening is that this can be realized by the well-known commercial software and, moreover, it performs well in estimating the number of independent components that are the original individual signals. In this study, those processes are used in ICA to extract the displacement of the structure and mode shape.

2.3 Algorithm of ICA

ICA is also referred to as Blind Source Separation, Blind Equalization, or Blind Beamforming depending on how to define the problem. In other words, this method is to

identify the mixed blind sources and unknown its mixing process that spark phenomenon. It is assumed that the blind sources also referred to as independent components are not correlated to each other. Based on statistically independent properties, the individual components and their traces of the mixture can be determined. In this sense, it is vital to define an objective function that enables one to measure the degree of the independence, e.g., Kullback–Leibler, Negentropy or Cumulant (Zang et al. 2004). Kurtosis is one of classical high-order approximations that is used to measure non-Gaussianity as expressed in Eq. (6).

$$\mathrm{kurt(X)} = \mathrm{E}\left\{\mathrm{X}^4\right\} - 3\left(\mathrm{E}\left\{\mathrm{X}^2\right\}\right)^2 \tag{6}$$

X is the vector composed of the non-Gaussian random variables representing the time history of the independent components and $E(O)$ is the expectation operator. In this study, ICA method that employs Kurtosis as the objective function and its application to mode decomposition from the structure's response are discussed. The linear relation between the structure's response and modal response is as bellow

$$Y = WX \tag{7}$$

Y is the structure's response, X is the modal response, and W is the linear transform matrix (mode shape). The key of ICA method is that the unknown variables X and Y are determined by the measurement Y. If W is a unitary square matrix and the inverse matrix W^{-1} exists, modal response X can be expressed as bellow

$$X = W^T Y \tag{8}$$

The matrix W and X can be determined by an iterative method minimizing the objective function in (6) until each mode is mutually independent. Equation (9) presents the updated matrix W.

$$W_{i+1} = E\left[Y\left(Y^T W_i\right)^{.3}\right] - 3W_i \tag{9}$$

$\mathrm{W_{i+1}}$ is the updated matrix W from the past $\mathrm{W_i}$ and the cubed term (3) in (9) stands for the cubed each element in the row vector $Y^T W_i$. Based on the assumption that the each of decomposed modes are equivalent to the response of the corresponding single degree of freedom systems, the natural frequencies and damping ratio are calculated. The viability of the ICA algorithm is evaluated in the following session with two examples.

3 Experimental Testing

3.1 Three-story Steel Frame

The three-story steel structure use for the modal testing is shown in Fig. 3. Each floor's mass is 18.62 kg and the height of each column is 400 mm long. The width and thickness of the column is 50 mm and 2.3 mm, respectively. Table 1 presents the dynamic properties of the structure and its analytical modal parameters. It is assumed that the mass at each floor is uniform and both ends of the columns between the floor are fully constrained with two effective lengths: 400 mm for full height and 350 mm for those without the right angle joint bracket.

The analytical modal analysis of the structure represents different natural frequencies, but uniform mode shapes. The errors between the results with two different column lengths for the first three modes are uniform equal to approximately 20%. The result is consistent with the stiffness increased by about 50% when the short columns are taken into account without change in mass. The uniform stiffness of all floors accounts for the identical mode shapes for two column lengths.

In the experiment, three accelerometers are installed at each floor to measure the mono-direction response and additional one as a reference on the ground is to detect the deformation of the moment resisting connections. The top floor is excited by an unknown input or blind source using an impact hammer shown in Table 2. The output signals by the impact at each floor and the contribution of each mode separated by spectral analysis are exhibited in Figs. 4 and 5, respectively. As seen, the first mode at the 3rd floor is dominant followed by the 2nd and 3rd mode and those three modes are superposed in the time history as shown in Fig. 4a. Similarly, the 1st and 2nd floor's accelerograms also appear to be influenced by three modal responses, while the second mode is of greater contribution to the 1st floor's response. The result of the spectral analysis is summarized in Table 3.

The natural frequency and mode shape are determined by picking the peaks of the spectra and the square root of the peak amplitude corresponding to each mode, respectively. The outcome of this example shows that the experimental modal parameters are in line with the analytical result of the structure with the shorter columns shown in Table 1. As for the mode shape, the first two modes shape for both analytical and experimental result are in good agreement, while the 3rd mode shape shows a little discrepancy. The error in mode shape between two results can be quantitatively examined using Mode Assurance Criteria value as below

$$MAC = \phi^T \bar{\phi} / \overline{\phi^T} \bar{\phi} \tag{10}$$

Φ is spectral mode shape and $\bar{\Phi}$ is analytical mode shape. The MAC values of the 1st, 2nd and 3rd mode shape are 1.6% and 3.26% and 12.11%, respectively. The peak picking method, however, in frequency domain holds significant uncertainties in practice. In this study, thus, Hilbert

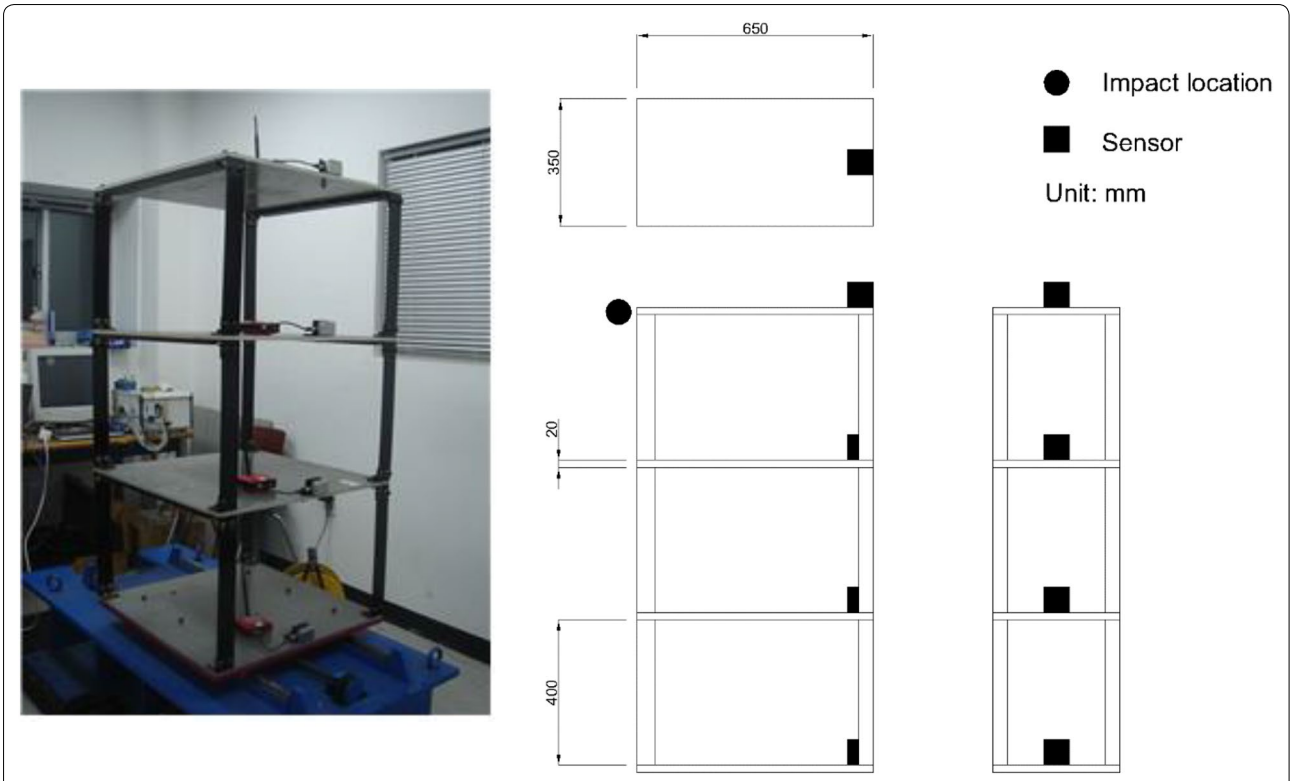

Fig. 3 Three-story steel structure.

Table 1 Dynamic parameters of the structure.

Floor mass	m = 18.62 kg		
Floor stiffness	$k = 4*12EI/L3$ = 7.7945 kN/m (L = 400 mm) = 11.635 kN/m (L = 350 mm)		
Mass matrix	$\begin{bmatrix} m & 0 & 0 \\ 0 & m & 0 \\ 0 & 0 & m \end{bmatrix}$	Stiffness matrix	$\begin{bmatrix} 2k & -k & 0 \\ -k & 2k & -k \\ 0 & -k & k \end{bmatrix}$
Modal parameters	Mode 1	Mode 2	Mode 3
Natural frequency			
L = 400	1.4492 Hz	4.0605 Hz	5.8676 Hz
L = 350	1.7706 Hz	4.9610 Hz	7.1689 Hz
Mode shape normalized to the top floor	0.4450	− 1.2467	1.8026
	0.8021	− 0.5547	− 2.2474
	1.0000	1.0000	1.0000

transform (Feldman 2011) together with ICA is exploited to determine the modal frequency and subsequently the robustness of this method is evaluated comparing with the classical methods such and pick peaking.

In this example, the output signal Y is the relative acceleration generated by the impact on the top floor of the steel structure with respect to the support at the bottom. The values of elements in the linear transform matrix W in Eq. (9) are those that are converged within the tolerance in the iterative process of updating the linear transform matrix W. In Table 4, the mode shapes of the structure are presented. W that consists of the mode shapes is unitary matrix and the column vectors are normalized for elements corresponding to the top floor to have unity. The difference in MAC values between ICA and analytical method is greater than that between ICA and spectral analysis and the discrepancy increases in the higher modes. Figure 6 displays the modal responses and spectral contents around each mode obtained by ICA. The decomposed time history by the three methods mentioned in this example are in good agreement with each other despite a small discrepancy in the mode shape amongst the methods. Meanwhile, the analytical spectrum shows slight discrepancy from those of the spectral analysis and ICA. However, those three methods identify three different modes effectively since the log-scale amplitude difference in three peaks lies between two and three orders in each mode's power spectrum plot.

Next, the natural frequency of identified modes is calculated. In order to calculate modal parameters, it is very useful to understand that the response of decomposed mode is equivalent to the SDOF system. In this sense, the natural frequency is obtained from the well-distributed

Table 2 Accelerometer and impact hammer.

Sensitivity	0.23 mV/N
Frequency range	0–5 kHz
Amplitude range	22 kN
Hammer mass	0.32 kg
Head diameter	25 mm
Hammer view	

peaks in the spectra in Fig. 6. However, it is not always simple to pick the peaks in practice due to the intrinsic uncertainties in the spectrum. Thus, Hilbert transform that employs the probability distribution of time-varying frequencies is used to determine the natural frequency.

In Fig. 7, Hilbert transform of the first modal response is used to extract instantaneous frequency and the distribution of the instantaneous frequency, cumulative distribution, and probability density function are plotted. As shown, most instantaneous frequencies of the first mode are between 0 and 3 Hz (a) and the mean value that corresponds to 0.5 in cumulative distribution function is equal to 1.7357 Hz (b). This first mode frequency is very close to the result of the spectral analysis. The curve in Fig. 8c is the probability density function obtained by taking the derivative of the cumulative density function. The distribution of the variable which is the natural frequency does not appear very smooth. Since this example produces very smooth cumulative distribution, using CD is sufficient to estimate the natural frequency. However, it is worth noting that using PDF may be more efficient than using CD in different type of structures. Similarly, the modal parameters of the second and third mode can be estimated through the above procedure. This study discusses only the first mode.

In Table 5, the natural frequency obtained by CD and the error in the resultant values between ICA and spectral analysis are presented. The insignificant level of error supports the effectiveness of the statistical approach of the instantaneous natural frequency by the Hilbert transform.

Not only the natural frequency, but also damping ratio can be calculated using Hilbert transform. Since the steel structure is subjected to the excitation by impact, the structure's response reaches the free steady-state vibration as the initial transient vibration subsides. Thus, the state equation of the linear system in free vibration is given by

$$\dot{x} = Axx(0) = x_0 \tag{11}$$

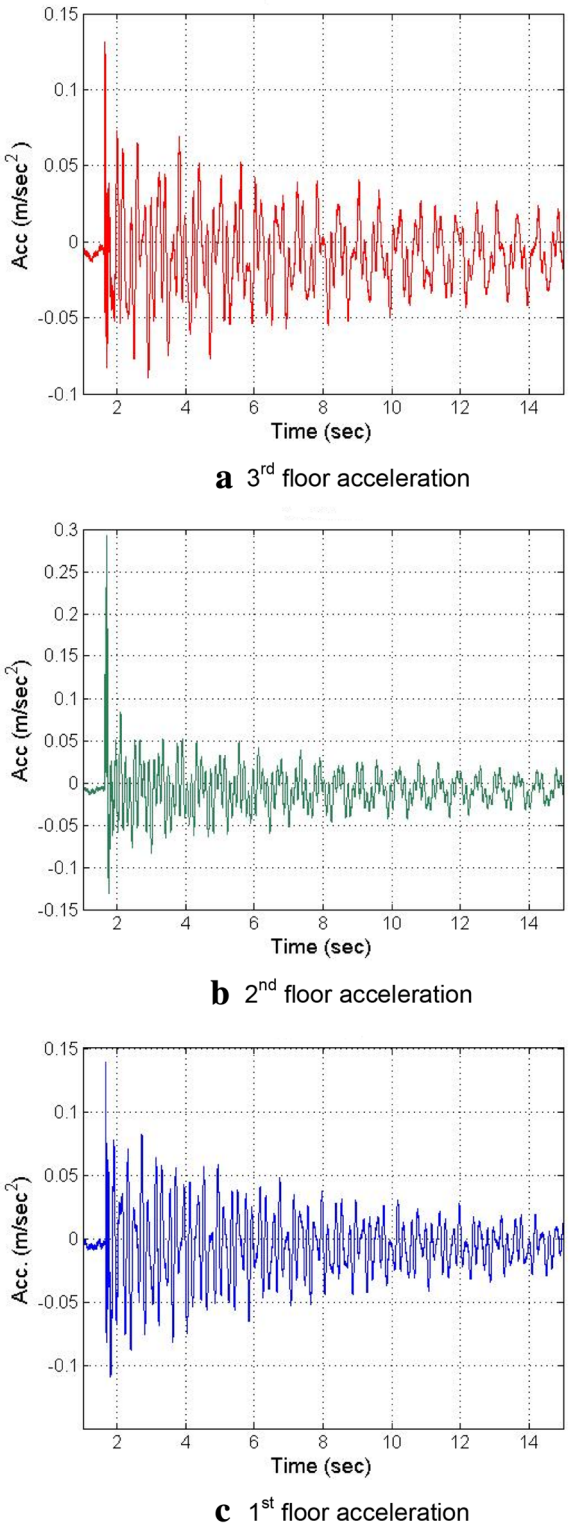

Fig. 4 The response by the impact excitation.

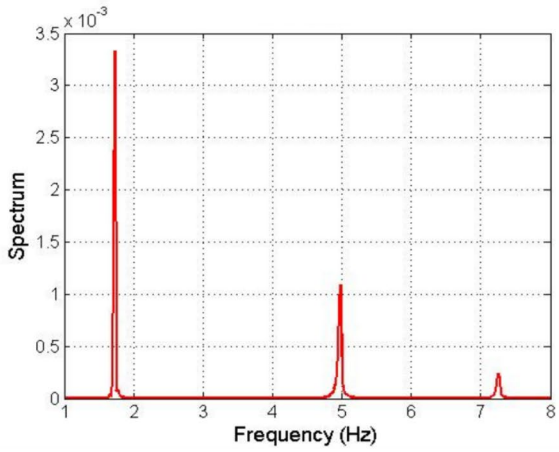

a 3rd floor acceleration

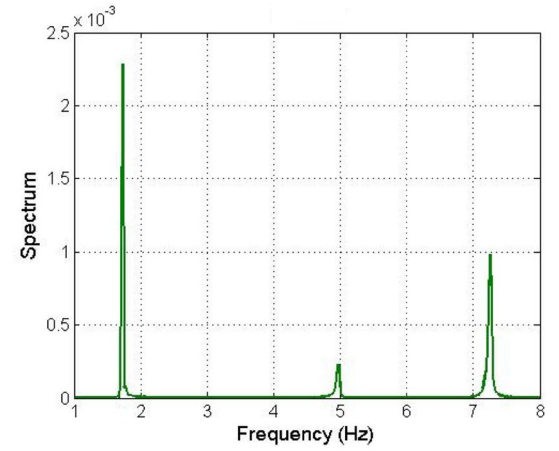

b 2nd floor acceleration

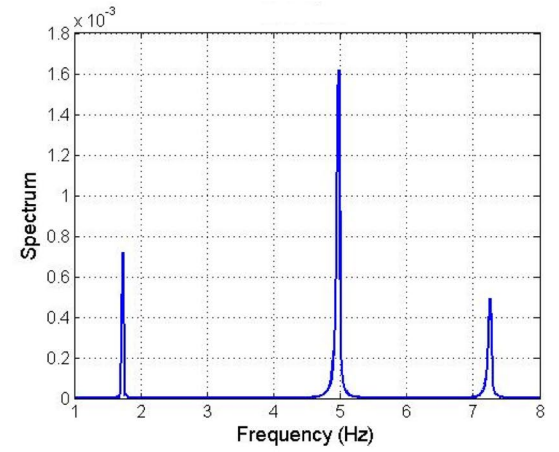

c 1st floor acceleration

Fig. 5 Response spectra.

Table 3 Modal parameters by spectral analysis.

	Mode 1	Mode 2	Mode 3
Natural frequency	1.7322 Hz	4.9824 Hz	7.2504 Hz
Normalized mode shape	0.4649	− 1.2203	1.4396
	0.8278	− 0.4459	− 2.0374
	1.0000	1.0000	1.0000

Table 4 The mode shapes by ICA method.

Method	Mode 1	Mode 2	Mode 3
ICA (1st–2nd–3rd floor)	0.4702	− 1.2009	1.4306
	0.8216	− 0.4192	− 1.8688
	1.0000	1.0000	1.0000
Analytical	0.4450	− 1.2467	1.8026
	0.8021	− 0.5547	− 2.2474
	1.0000	1.0000	1.0000
MAC ICA Vs. Analytical	1.46%	− 4.62%	− 16.36%
Peak picking(PP)	0.4649	− 1.2203	1.4396
	0.8278	− 0.4459	− 2.0374
	1.0000	1.0000	1.0000
MAC ICA Vs. PP	− 0.14%	− 1.33%	− 4.93%

x_o is the unknown initial value, A is the system matrix expressed as

$$A = \begin{bmatrix} 0 & 1 \\ -\omega^2 & -2\xi\omega \end{bmatrix} \tag{12}$$

ω and ξ are the natural frequency and damping ratio of each mode, respectively. If the covariance of the system response x is $P = E[xx^T]$, the relationship between P and A can be written as

$$\dot{P} = PA^T + AP \tag{13}$$

At this stage, the state variables for the displacement and velocity of the system are still unknown, but only the output signal that is measured acceleration is available. The output y can be expressed as

$$y = Cx \tag{14}$$

The Hilbert transform of the output signal y and the state variable x can be also expressed as

$$y_H = Cx_H \tag{15}$$

The relationship between output signal and the covariance of its Hilbert transform can be written as

$$C\dot{P}_H C^T = CAP_H C^T + CP_H A^T C^T \tag{16}$$

If the eigenvalue λ of the system matrix that satisfies the relationship $CAx = \lambda Cx$ is present, the covariance including the Hilbert transform can be expressed as

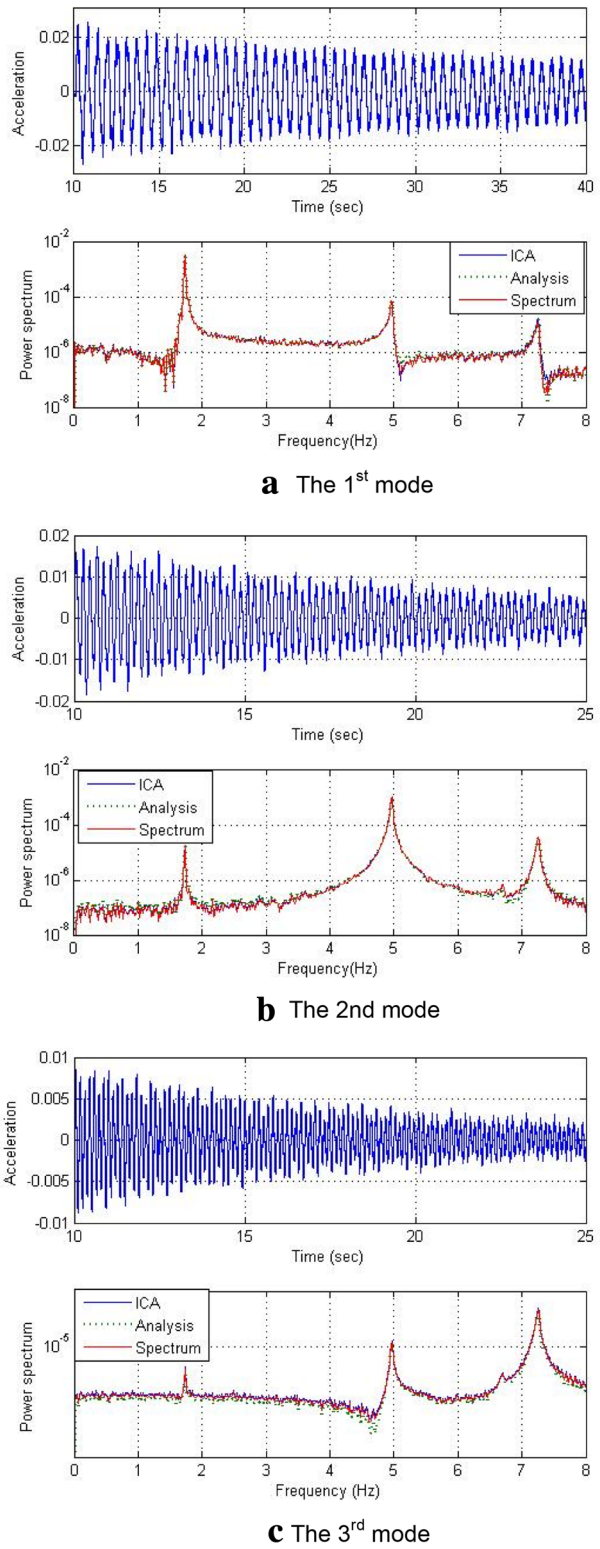

Fig. 6 The decomposed modal response and spectra.

$$\dot{P}_y = \lambda P_y + P_y\tilde{\lambda} = 2Re(\lambda)P_y \tag{17}$$

$Re(\lambda)$ is the real part of λ and is equal to $-\omega\lambda$. Consequently, the covariance of the output P_y and its square root which is standard deviation Sy can be obtained.

$$P_y = e^{-2\omega\xi t}P_{y_0} \tag{18a}$$

$$S_y = \sqrt{P_y} = e^{-\omega\xi t}S_{y_0} \tag{18b}$$

where P_{y_0} is the unknown initial value of the covariance P_y.

Figure 8 shows the instantaneous standard deviation (the square root of the covariance) of the third mode response and the estimation using Eq. (18b). The logarithmic decrement of the time history is also illustrated in the dotted line to show the conventional damping ratio evaluation. In this estimation, the natural frequency in Table 5 is used and the unknown initial covariance and damping ratio is obtained using the least square method represented in the continuous red line. Similarly, the damping ratio of three modes are calculated and presented parallel with those by the classical method in Table 6. The estimated damping ratio by Hilbert transform of all modes is measured 0.3% and the error with respect to the logarithmic decrement ranges from −3 to 4%. This discrepancy range is regarded as insignificant value. Therefore, above example indicates that the damping of the system can be effectively estimated by the change in the covariance derived from Hilbert transform of output.

3.2 High-rise Building Subjected to Strong Wind Load

In recent tall buildings, coupled torsional-translational behavior is observed. As the structure is subjected to unidirectional translational wind load, for instance, usually two translational responses in parallel and perpendicular direction to the load and torsional response are observed. To be specific, a few lower modes are blended in torsional-translational modes and those individual modes other have different contribution to the global behavior of the structure. The natural frequencies of those modes comprising the coupled behavior are often so close that the modal identification requires more delicate approach to separate them clearly (Kareem 1985).

In this example, the ICA technique discussed above is applied to decompose the close modes in the coupled motion of the existing 39-story building and validation of the technique is performed. For dynamic identification,

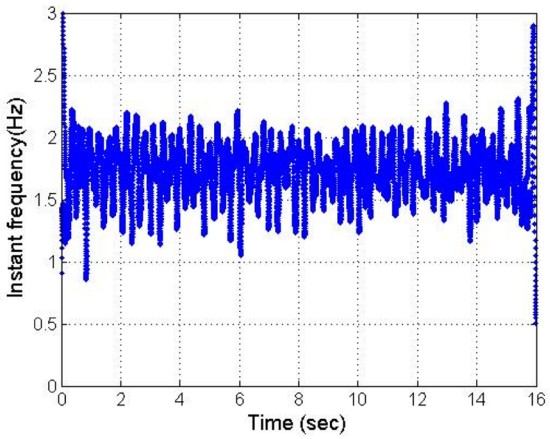

a Instantaneous natural frequency by Hilbert transform

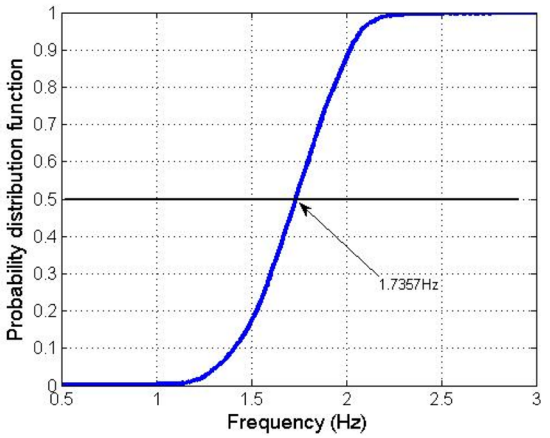

b Cumulative distribution function (mean frequency: 1.7357 Hz)

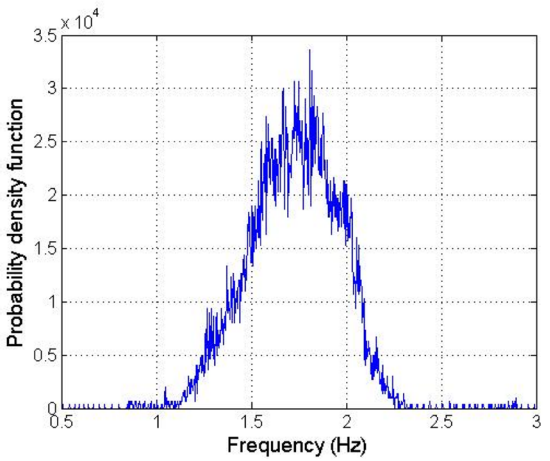

c Probability density function of instantaneous frequency

Fig. 7 The natural frequency distribution of the first mode.

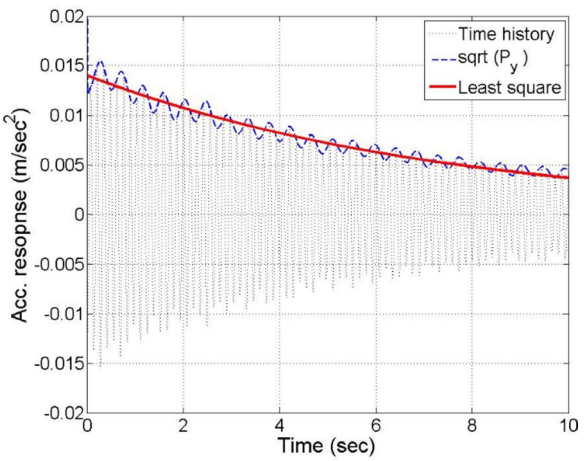

Fig. 8 The covariance of the third mode response and its estimation.

Table 5 The identified natural frequencies.

Method	Mode 1 [Hz]	Mode 2 [Hz]	Mode 3 [Hz]
ICA (Cumulative distribution)	1.7357	4.8043	7.1150
Peak-picking	1.7322	4.9824	7.2504
Error	0.2%	− 3.57%	− 1.87%

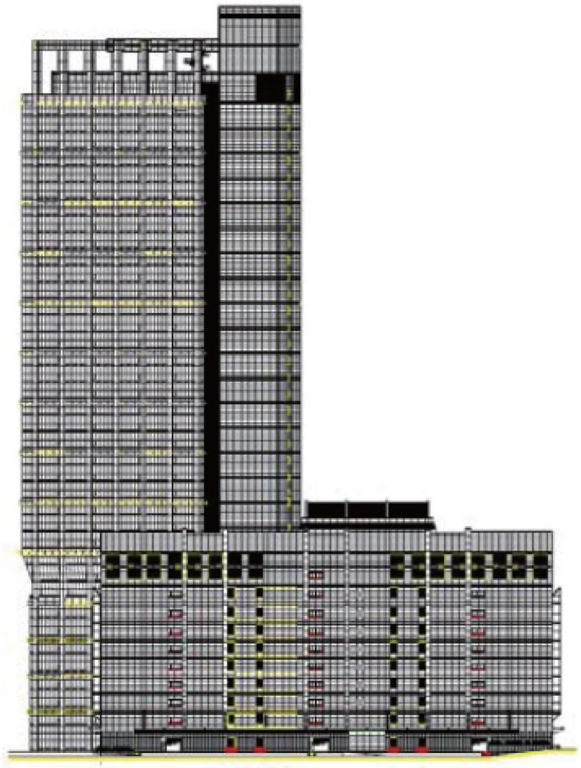

Fig. 9 The 39-story building.

Table 6 Damping estimation using the derivative of the covariance.

Method	Mode 1	Mode 2	Mode 3
Covariance	0.25%	0.35%	0.3%
Logarithmic decrement	0.24%	0.36%	0.29%
Error	+ 4%	− 3%	3%

the acceleration signals recorded at three different locations on the top floor while a typhoon took place are used.

The steel-reinforced concrete mixed skyscraper is located in Seoul, South Korea and has 39 floors (188 m). Its construction was complete in 1998 and the building has commercial and entertainment use. Figure 9 represents the building of the experiment. Wind-induce vibration was measured at the 38th floor (160 m) from 5:00 a.m. until 3:00 p.m. in August 8th in 2011 using the accelerometers indicated position A and B in Fig. 10. The distance between A and B is 13 m.

In Fig. 11, the three-axis acceleration signals measured at location B in the morning is exhibited. The peak acceleration is approximately 2 cm/sec^2 and it is observed that waveforms in X and Y direction are slightly different. Next, X- and Y-direction vibrations at two locations recorded in the afternoon are displayed in Fig. 12. Instead of the vertical Z-direction response, two Y-direction time history were recorded to observe the torsional behavior of the plane. As shown, the amplitude of the Y-direction responses is greater than that in X direction and the Y-direction acceleration of A near the edge is greater than that of B. The peak acceleration in this period is 3.94 cm/sec^2.

First, the signals of each direction are examined by spectral analysis. As pre-processing, zero-mean process, noise cancelling and low pass filter with cut-off frequency of 5 Hz were introduced to the time series. The processed time history of Y-direction accelerations and corresponding spectra are presented in Fig. 13. As mentioned previously, the peak amplitude at A (y2) almost doubles that at B (y1). In the spectrum, the major vibration modes in Y direction can be found near 0.2 Hz and 0.3 Hz and the spectral amplitude of y2 at 0.3 Hz outnumbers that of y1. This difference explicitly implies that the 0.3 Hz mode is most likely the fundamental torsional mode. Meanwhile, the spectrum of the x-direction signal illustrated in Fig. 14 represents a new mode near 0.22 Hz which is as significant as the mode near 0.2 Hz, while the amplitude near 0.3 Hz which is supposed to be the torsional

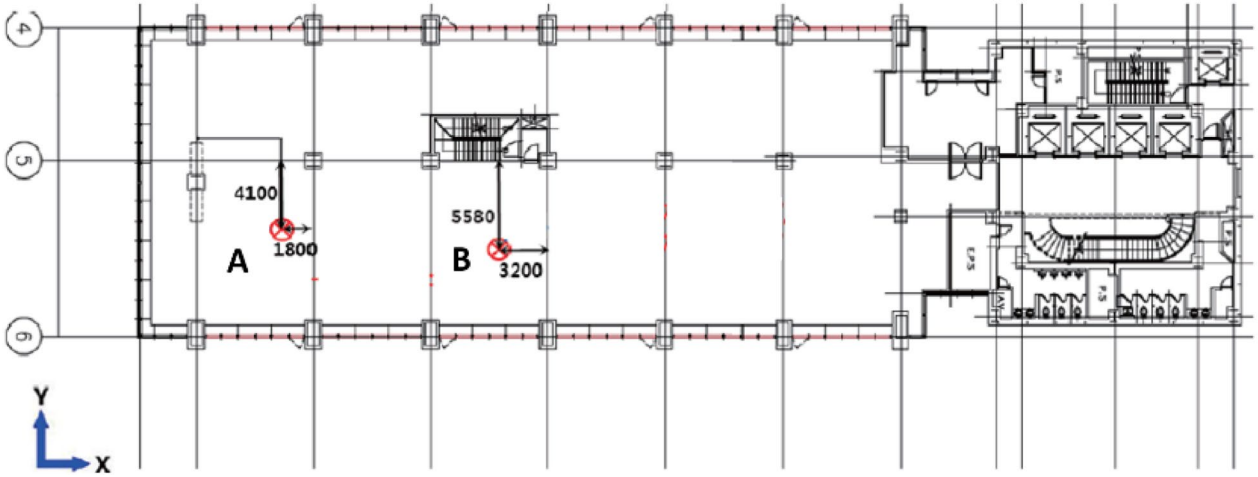

Fig. 10 Plan view of the top floor and measurement layout.

mode is very small. At this point three modes near 0.2, 0.22, and 0.3 Hz are loosely identified by the basic peak picking method. However, those frequencies can vary with the parameters considered in the spectral analysis as discussed in the first example. Subsequently, the probable three modes are separated by ICA.

First, the mode shapes are given by the linear transform matrix produced by the mode decomposition procedure of ICA. The modes other than first three modes are so insignificant that those are neglected in this example. The decomposed time history corresponding to mode 1, 2, and 3 and their spectra are shown in Fig. 15. The clearly different waveforms of each separate time series account for little correlation between the modes. It should be noted that the value of the decomposed responses calculated by ICA is dimensionless such that the values in the y-axis of the time domain in Fig. 15 does not show physical quantity, but only relative amplitude. Thus, the linear transform matrix A is required for the outcome of ICA to be converted into the acceleration with unit. The components of transform matrix A and corresponding mode shapes are presented in Table 7 and Fig. 16, respectively.

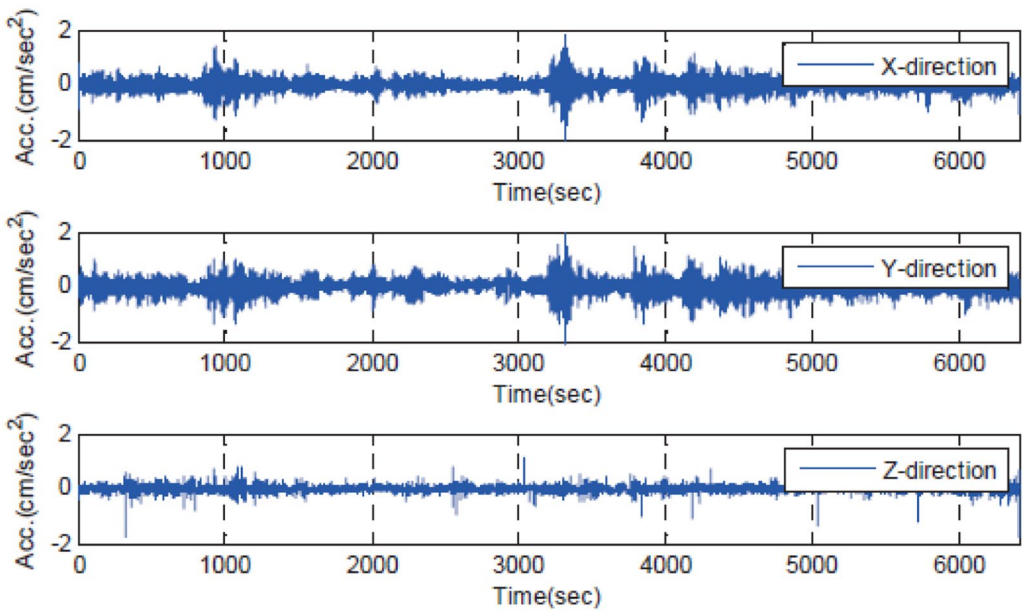

Fig. 11 Accelerograms at B.

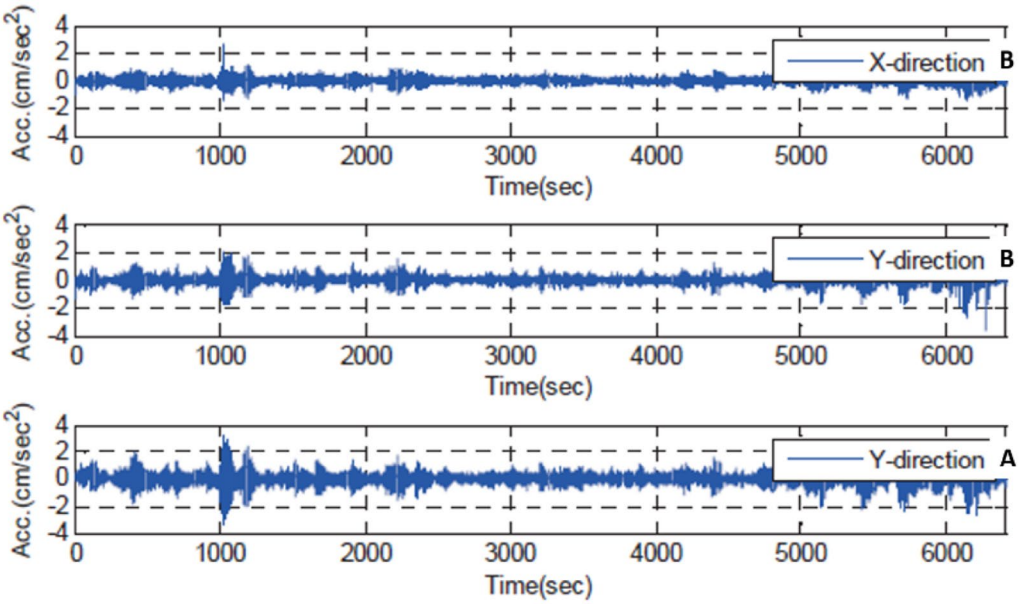

Fig. 12 Accelerograms at A and B.

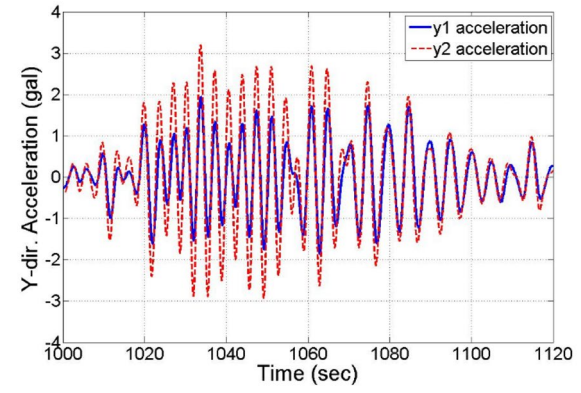

a Time history

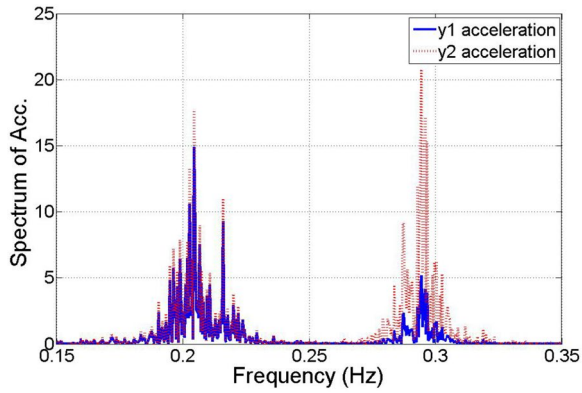

b Spectrum

Fig. 13 Wind induced accelerations in Y direction.

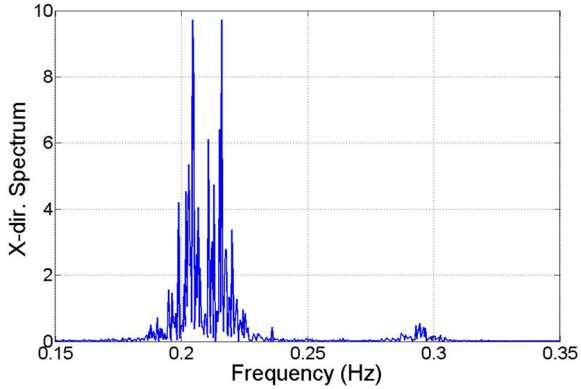

Fig. 14 Spectrum of X-direction signal.

Very little effect of torsion is found in mode 1 and 2. Regarding translational behavior, mode 1 represents almost equal effect on both X-and Y-direction response, while the effect in Y direction is pronounced in the second mode shape. As predicted, a remarkable torsional mode shape is shown in mode 3.

It is worth mentioning that there might be a trade-off between neglecting higher insignificant modes to facilitate ICA decomposition and a loss of a part of original data. Application of filters can also result in data loss when restoring original data. For this reason, it is necessary to assess the level of signal distortion and loss caused by mode separation by ICA. It can be achieved

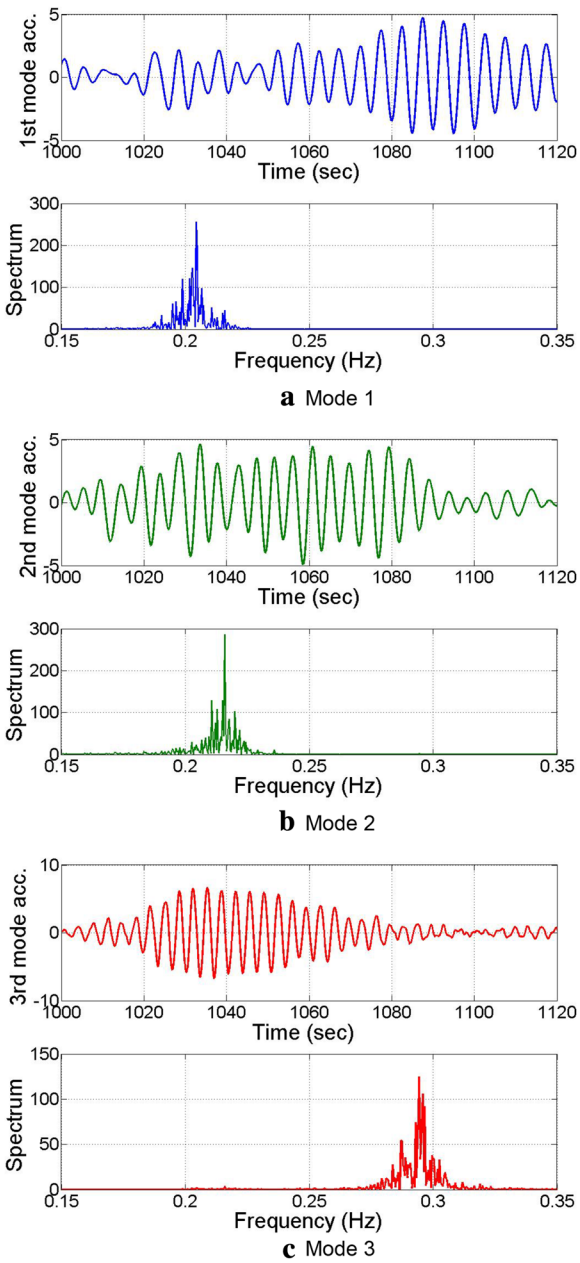

Fig. 15 Decomposed modes and spectra.

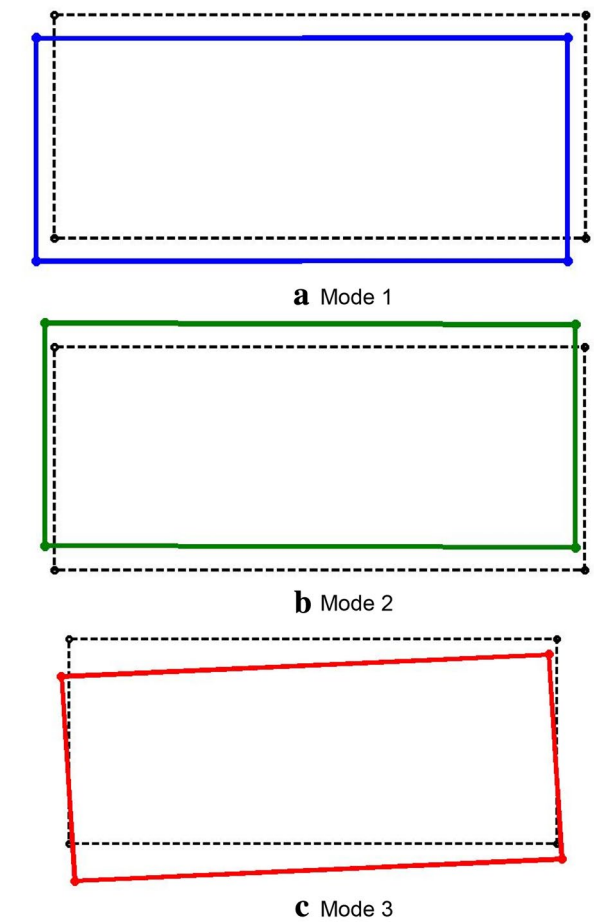

Fig. 16 Mode shape of the tall building by ICA.

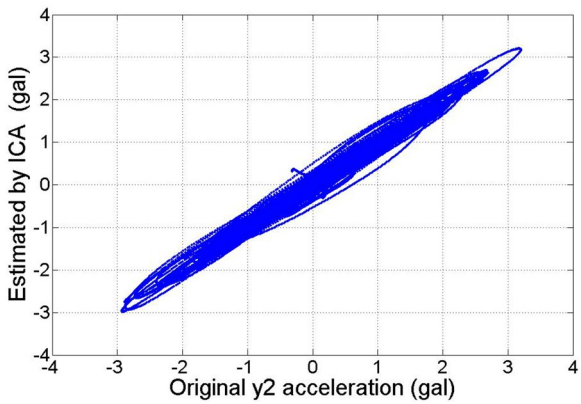

Fig. 17 Correlation between the original and restored signal (correlation coefficient: 0.985).

Table 7 Transform matrix and mode shape.

		Mode 1	Mode 2	Mode 3
Transform matrix A	X	−0.2036	−0.1065	0.0649
	Y1 at B	−0.2011	0.2060	−0.1505
	Y2 at A	−0.2058	0.2187	−0.3624
Transform relationship	Z = AS where *Z*: measured output S: dimensionless response by ICA			

by converting the non-dimensional decomposed modes into acceleration quantities according to the relation given in Table 7. The correlation between the restored

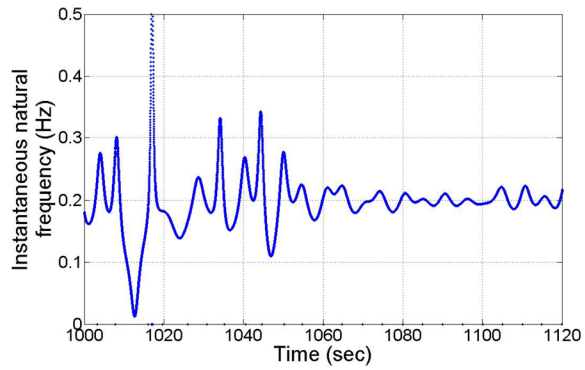

Fig. 18 Instantaneous natural frequency of mode 1.

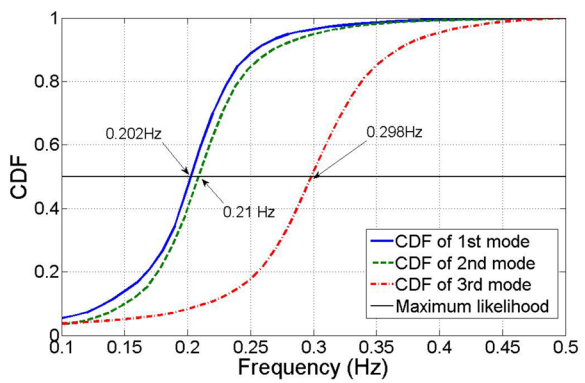

Fig. 19 Cumulative distribution function of time-varying natural frequency.

acceleration by combining three separate time histories from ICA and the original output of y2 is illustrated in Fig. 17. As seen, two time series are in good agreement and its correlation coefficient is equal to 0.985. Therefore, this result strongly supports that ICA is a stable modal decompostion technique and is of great potential in operational modal analysis for the large-scale structures subjected to random vibration.

Finally, the natural frequencies of each mode are estimated using Hilbert transform as previous example. The separate natural frequencies shown in Fig. 15 are still ambiguous and furthermore the unknown frequencies of the wind load mixed with building's natural frequencies makes identification more difficult. The instantaneous natural frequency of mode 1 by Hilbert transform with respect to time obtained is represented in Fig. 18. It is shown that most time-varying natural frequencies are found between 0.1 and 0.3 Hz and this distribution implies uncertainty. When the distribution is, however, displayed as a function of cumulation as shown in Fig. 19, the most frequent variable, which is natural frequency in this problem, is specified at CDF 0.5: 0.202 Hz, 0.21 Hz, and 0.298 Hz for mode 1, 2, and 3, respectively. Although those natural frequencies are so close that they cannot be separately by peak picking technique, ICA and Hilbert transform can decouple the combined vibration modes and identify modal parameters efficiently.

4 Conclusions

In this study, ICA method designed for mode decomposition is validated via experiments using a scaled structural model. The findings of the validation are summarized as follows:

1) Based on the robust mathematical model, ICA is an effective method to evaluate mode shapes from the output-only signal of the structure. The mode shapes obtained by ICA method agree with those by the analytical and peak picking methods.
2) Two modal identification examples show that the ICA technique allows one to decompose structural response into individual modes even if the modes are very close. The natural frequency and damping ratio can be also calculated from each identified mode by a statistical approach. Closely spaced modes in a coupled torsional translational behaviour induced by non-gaussian excitation such as strong wind loads on a high-rise building are successfully identified. The ICA and Hilbert transform-based scheme can identify explicitly modal parameters of existing buildings.
3) Another advantage of using ICA is verified by reversing the separate modes obtained by ICA. The restoring of the outcome of ICA results in the original output signal without any deterioration in the data quality.
4) Complementary study to reduce the statistical error in the estimation of natural frequency due to unknown dynamic properties the excitation.

Abbreviations

α: basis; λ: eigenvalue; ξ: damping ratio; φ: spectral mode shape; $\bar{\Phi}$: analytical mode shape; ω: natural frequency; A: matrix consisting for column vectors $\alpha(i)$; C: transform matrix between output y and state variable x; D: diagonal matrix comprised of eigen values λ; E: orthogonal matrix comprised of eigen vectors; *kurt*: kurtosis; m: the number of signals; *MAC*: mode assurance criteria; $\widehat{N}$: noise; P: expectation of xx^T; P_y: covariance of the output; P_{y_0}: unknown initial value of the covariance P_y; $\dot{P}_y$: derivative of covariance of the output; *Re*: real part of complex number; s: original signal; *Sy*: standard deviation; t: time step; W: linear transform matrix; x: mixed system response signal; x_H: Hilbert transform of state variable x; X: modal response; $\bar{x}$: mean value of x; x^*: zero mean value of x; $\dot{x}$: State variable; *xo*: unknown initial value; y: output signal; Y: structure's response; y_H: Hilbert transform of output y.

Authors' contribution
JH improved the ICA method and programmed its algorithm for the analysis used in the examples. JH, JN and SL conducted experimental studies, outlined the structure of the paper and drafted the manuscript. AK participated in the review and verification of the proposed methods in this paper and drafting the manuscript. All authors read and approved the final manuscript.

Author details
[1] School of Architecture, Chonnam National University, 77 Yongbong-ro, Buk-gu, Gwangju 61186, Republic of Korea. [2] Department of Planning and Design in Complex Environments, IUAV University of Venice, 2206, Dorsoduro, 30123 Venice, Italy. [3] Department of Architectural Engineering, Dankook University, 152, Jukjeon-ro, Suji-gu, Yongin-Si, Gyeonggi-do 16890, Republic of Korea. [4] NatHaz Modeling Laboratory, Department of Civil & Environmental Engineering and Earth Sciences, University of Notre Dame, Notre Dame, IN 46556, USA.

Acknowledgements
This research was financially supported by the Basic Science Research Program of the National Research Foundation of Korea (NRF), Grant No. NRF-2017R1D1A1B03031265 and No. NRF-2015R1A2A1A10054506. The third author was in part supported by NSF Grant No. GMMI1612843.

Competing interests
The authors declare that they have no competing interests.

Publisher's Note

Received: 9 August 2018 Accepted: 11 November 2018
Published online: 07 January 2019

References

Alvandi, A., & Cremona, C. (2006). Assessment of vibration-based damage identification techniques. *Journal of Sound and Vibration, 292,* 179–202.

Bee, M., & Micheyl, C. (2008). The cocktail party problem: What is it? How can it be solved? And why should animal behaviorists study it. *Journal of Comparative Psychology, 122*(3), 235–251.

Brincker, R., Zhang, L., & Andersen, P. (2002). Modal identification of output-only systems using frequency domain decomposition. In: *Proc. of IMAC18* (pp. 625–630). San Antonio, Texas, USA.

Cichocki, A. (2004). Blind signal processing methods for analyzing multichannel brain signals. *International Journal of Bioelectromagnitism, 6*(1), 22–27.

Du N, Bai G, Xu Y, Qin C. Experimental and Numerical Researches on the Seismic Behavior of Tubular Reinforced Concrete Columns of Air-Cooling Structures. Inter J Concr Struct Mater. 2017;11(3):459–75.

Feeny, B. (2002). On proper coordinates as indicator of modal activity. *J Sound and Vibration, 255,* 805–817.

Fortuna, J., & Capson, D. (2002). ICA for position and pose measurement from images with occlusion. In: *IEEE international conference on acoustics, speech, and signal processing*.

Guo, Y., & Kareem, A. (2015). System identification through nonstationary response: Wavelet and transformed singular value decomposition—Based approach. *Journal of Engineering Mechanics, 141,* (7).

Guo, Y., & Kareem, A. (2016a). Non-stationary frequency domain system identification using time–frequency representations. *Mechanical Systems and Signal Processing, 72–73,* 712–726.

Guo, Y., & Kareem, A. (2016b). System identification of nonstationary data using time-frequency blind source separation. *Journal of Sound and Vibration, 371,* 110–131.

Guo, Y., Kwon, D. K., & Kareem, A. (2016). Near-real-time hybrid system identification framework for civil structures with application to Burj Khalifa. *Journal of Structural Engineering, 142*(2), 04015132.

Han, S., & Feeny, B. (2003). Application of proper orthogonal decomposition to structural vibration analysis. *Mechanical System and Signal Processing, 17,* 989–1001.

Haykin, S., & Chen, Z. (2005). The cocktail party problem. *Neural Computation, 17,* 1875–1902.

Hazra, B., Roffel, A. J., Narasimhan, S., & Pandey, M. D. (2010). Modified cross-correlation method for the blind identification of structures. *Journal of Engineering Mechanics, 136*(7), 889–897.

Feldman, M. (2011) *Hilbert Transform applications in mechanical vibration*. New York: John Wiley & Sons, Inc.

Hwang, J. S., Kwon, D. K., & Kareem, A. (2018). Estimation of structural modal parameters under winds using a virtual dynamic shaker. *Journal of Engineering Mechanics, 144,* (4).

Hyvaerinen, A., Karhunen, J., & Oja, E. (2001). *Independent component analysis*. New York: John Wiley & Sons, Inc.

Hyvaerinen, A., & Oja, E. (2000). Independent component analysis: Algorithm and applications. *Neural Networks, 13*(4–5), 411–430.

Kareem, A. (1985). Lateral-torsional motion of tall buildings to wind loads. *Journal of Structural Engineering, 111*(11), 2479–2496.

Lee, T. W. (1998). *Independent component analysis: Theory and applications*. Boston: Kluwer Academic Publications.

Lee J, Park Y, Jung C, Kim J. Experimental and Measurement Methods for the Small-Scale Model Testing of Lateral and Torsional Stability. Inter J Concr Struct Mater. 2017;11(2):377–89.

Madhow, U. (1998). Blind adaptive interference suppression for direct-sequence CDMA. *Proceedings of the IEEE, 86*(10), 2049–2069.

McNeill, S. I., & Zimmerman, D. C. (2010). Relating independent components to free-vibration modal responses. *Shock and Vibration, 17*(2), 161–170.

Nagarajaiah, S., & Yang, Y. (2013). Time-frequency blind source separation using independent component analysis for output-only modal identification of highly damped structures. *Journal of Structural Engineering, 139*(10), 1780–1793.

Nagarajaiah, S., & Yang, Y. (2015). Blind modal identification of output-only non-proportionally-damped structures by time-frequency complex independent component analysis. *Smart Structures and Systems, 15*(1), 81–97.

Peeters, B., & De Roeck, G. (1999). Reference-based stochastic subspace identification for output-only modal analysis. *Mechanical Systems and Signal Processing, 13*(6), 855–878.

Poncelet, F., Kerschen, G., Golinval, J. C., & Verhels, D. (2007). Output-only modal analysis using blind source separation techniques. *Mechanical Systems and Signal Processing, 21,* 2335–2358.

Reynders, E. (2012). System identification methods for (operational) modal analysis: Review and comparison. *Archives of Computational Methods in Engineering, 19,* 51–124.

Sadhu, A., Narasimhan, S., & Antoni, J. (2017). A review of output-only structural mode identification literature employing blind source separation methods. *Mechanical Systems and Signal Processing, 94,* 415–431.

Wu, J. (2011). Estimating source kurtosis directly from observation data for ICA. *Signal Processing, 91*(5), 1150–1156.

Yang, Y., & Nagarajaiah, S. (2013). Blind modal identification of output-only structures in time-domain based on complexity pursuit. *Earthquake Engineering and Structural Dynamics, 42*(13), 1885–1905.

Yang, Y., & Nagarajaiah, S. (2014). Blind identification of damage in time-varying systems using independent component analysis with wavelet transform. *Mechanical Systems and Signal Processing, 47*(1–2), 3–20.

Yang, Y., Nagarajaiah, S., & Ni, Y. (2015). Data compression of very large-scale structural seismic and typhoon responses by low-rank representation with matrix reshape. *Structural Control and Health Monitoring., 22*(8), 1119–1131.

Yang, K., Yu, K., & Li, Q. (2013). Modal parameter extraction based on Hilbert transform and complex independent component analysis with reference. *Mechanical Systems and Signal Processing, 40,* 735–802.

Zang, C., Friswell, M. I., & Imregun, M. (2004). Structural damage detection using independent component analysis. *Structural Health Monitoring, 3,* 69–83.

Zhang, L., & Brincker, R. (2005). An overview of operational modal analysis: Major development and issues. In: *Proceedings of the 1st international operational modal analysis conference* (pp. 179–190). Copenhagen: Aalborg University.

Zhou, W., & Chelidze, D. (2007). Blind source separation based vibration mode identification. *Mechanical Systems and Signal Processing, 21,* 3072–3087.